Observation of a Saharan dust outbreak on 1-2 August 2007: determination of size and microphysical particle parameters

Paolo Di Girolamo[1], Donato Summa[1], Rohini Bhawar[1], Tatiana Di Iorio[2], Marco Cacciani[2], Igor Veselovskii[3], Alexey Kolgotin[3]

[1]*DIFA, Università degli Studi della Basilicata, Potenza, Italy, Email: digirolamo@unibas.it*
[2]*Dipartimento di Fisica, Università degli Studi di Roma "La Sapienza", Roma, Italy, Email: tatianadiiorio@gmail.com*
[3] Physics Instrumentation Center, Troitsk, Moscow Region, 142190, Russia, E-mail: *igorv@pic.troitsk.ru*

ABSTRACT

The Raman lidar system *BASIL* was operational in Achern (Black Forest) between 25 May and 30 August 2007 in the frame of the Convective and Orographically-induced Precipitation Study (*COPS*). The system performed continuous measurements over a period of approx. 36 hours from 06:22 UTC on 1 August to 18:28 UTC on 2 August 2007, capturing the signature of a severe Saharan dust outbreak episode. Data clearly reveals the presence of the dust cloud between 18:00 and 03:00 UTC, with the presence of two almost separate aerosol layers: a lower layer located between 1.5 and 3.5 km and an upper layer extending between 3.0 and 6.0 km.

An inversion algorithm was used to retrieve particle microphysical parameters, i.e., mean and effective radius, number, surface area, and volume concentration, complex refractive index, as well as the parameters of a bimodal particle size distribution, from the multi-wavelength lidar data of particle backscattering, extinction and depolarization. The retrieval scheme employs Tikhonov's inversion with regularization and makes use of Mie kernel functions for spheroidal particles. Parameters of dust particles are estimated as a function of altitude at different times during the dust outbreak event. Retrieval results reveal the dominance in the upper dust layer of a coarse mode with radii 3-6 μm. Effective radius, number density and volume concentration vary with altitude in the range 0.1-1.4 μm, 200-1500 cm^{-3} and 6-80 $\mu m^3/cm^3$, respectively, while real and imaginary part of the complex refractive index are in the range 1.45-1.62 and 0.005-0.012, respectively.

1. INTRODUCTION

The Sahara desert is the most important global source of aeolian dust [1]. Dust is exported from the Sahara in discrete outbreaks of several days' duration, with location and direction shifting with the seasonal movement of the Intertropical Convergence Zone [2]. The annual peak in outbreak activity usually occurs in late winter and spring [3]. The inter-annual variability of the dust export to the Atlantic and Mediterranean regions is controlled by large-scale processes, as the North Atlantic Oscillation and Sahelian rainfall [5].

The present paper reports Raman Lidar measurements performed during an unusually strong and large-scale Saharan dust outbreak event that occurred in late July 2007 and affected a major area in Southern and Central Europe. Global and mesoscale models predicted large precipitations episodes for 2 August 2007 in the region of measurements. However, observed precipitations were far less intense than predicted. The lower amount of precipitation with respect to forecast is probably associated with the inadequateness of dynamical models to deal with desert dust radiative properties and their effects on cloud microphysics. Improvements in precipitation forecast can be obtained through the use of a dust prognostic scheme rather than a climatology or no dust effect at all [5].
Lidar measurements reported in this paper document the arrival and evolution of the desert dust cloud over a measurement site located in Achern, Southern Germany. Dust particles size and microphysical parameters are determined from multi-wavelength lidar measurements of particle backscattering coefficient, extinction coefficient and depolarization based on the application of a retrieval scheme employing Tikhonov's inversion with regularization. This recently developed scheme considers kernel functions for spheroidal particles in contrast with traditional Mie scattering schemes assuming particles with spherical shape.

2. BASIL

The measurements illustrated in this paper were performed by the Univ. of BASILicata Raman lidar system (*BASIL)* in the framework of *COPS – Convective and Orographically-induced Precipitation Study* - held in the period 01 June-31 August 2007. *BASIL* was deployed throughout the duration of COPS in Supersite R (Achern, Rhine Valley, Lat: 48.64 ° N, Long: 8.06 E, Elev.: 140 m). *BASIL* operated between 25 May and 30 August 2007 and collected more than 500 hours of measurements, distributed over 58 measurement days.

The major feature of *BASIL* is represented by its capability to perform high-resolution and accurate measurements of atmospheric temperature and water vapour, both in daytime and night-time, based on the application of the rotational and vibrational Raman lidar techniques in the UV. Besides temperature and water vapour, *BASIL* is capable to provide measurements of particle backscatter at 355, 532 and 1064 nm, particle extinction coefficient at 355 and 532 nm and particle depolarization at 355 and 532 nm [6].

The implementation of the particle backscatter measurement capability at 1064 nm was made possible thanks to the cooperation with the University of Rome "La Sapienza". For the purpose of determining particle size and microphysical parameters, measurements of the particle backscattering coefficient at 355, 532 and 1064 nm ($\beta_{355}(z)$, $\beta_{532}(z)$ and $\beta_{1064}(z)$), of the particle extinction coefficient at 355 and 532 nm ($\alpha_{355}(z)$ and $\alpha_{532}(z)$) and of the depolarization ratio at 355 nm ($\delta_{355}(z)$) are used.

© Proceedings of the 8th International Symposium on Tropospheric Profiling, ISBN 978-90-6960-233-2
Delft, The Netherlands, October 2009. Editors, A. Apituley, H.W.J. Russchenberg, W.A.A. Monna

3. RETRIEVAL METHODOLOGY

The retrieval algorithm considered in this paper was recently developed at the *Physics Instrumentation Centre*. The considered algorithm represents the evolution of the retrieval schemes developed by Müller *et al.* [7] and Veselovskii *et al.* [8]. These former schemes were demonstrated to lead to an accurate determination of particle size distribution parameters based on the knowledge of five optical coefficients (particle backscattering coefficient at 355, 532 and 1064 nm and particle extinction coefficient at 355 and 532 nm, so called 3 β + 2 α approach). The schemes by Müller *et al.* [7] and Veselovskii *et al.* [8] assume the sounded particles to be spherical and solve the inverse problem using Mie kernel functions for spherical particles.

However, dust particles have predominantly non-spherical shapes, which render the standard Mie theory not applicable to compute their scattering properties. Thus, the application of the above inversion scheme to dust measurements may lead to significant errors in the retrieval of particle size and microphysical parameters. The possibility of using shape mixtures of randomly oriented spheroids for modelling light scattering by desert dust aerosol has been considered by several authors (among others, [9]).

At any height, the measured optical quantities g_i (backscattering or extinction) are related to the particle size distribution *f(r)* through the Fredholm integral equation:

$$\int_{r_{\min}}^{r_{\max}} K_i(m,\lambda,r) f(r) dr = g_i \quad i=1,..,L$$

where L is the number of measured optical quantities and $K_i(m,r,\lambda)$ are the kernel functions dependent on complex refractive index m, particle size r and wavelength λ. $K_i(m,r,\lambda)$ can be expressed as:

$$K_i(m,\lambda,r) = (1-\varphi)K_i^s(m,\lambda,r) + \varphi K_i^{un}(m,\lambda,r)$$

where ϕ is the spheroid fraction volume and $K_i^s(m,\lambda,r)$ and $K_i^{un}(m,\lambda,r)$ are the kernel functions for spherical and spheroidal particles, respectively. $K_i^{un}(m,\lambda,r)$ can be calculated through the look-up tables provided by Dubovik et. al, [10].

4. RESULTS

BASIL operated continuously over the 36 hour period from 06:22 UTC on 1 August to 18:28 UTC on 2 August 2007 to cover COPS IOPs 13a-b, primarily dedicated to the study of high pressure and forced convection. Figure 1 illustrates the time evolution of the particle backscatter ratio at 1064 nm, $R_{1064}(z)$, over a period of approx. 21 hours from 06:00 UTC on 1 August 2007 to 03:00 UTC on 2 August 2007. Lidar measurements captured the signature of a severe Saharan dust outbreak event. The dust cloud was found to reach the observation site around 11 UTC on 1 August. Marked evidence of the dust cloud is observed between 18 and 03 UTC, with the appearance of two almost separate aerosol layers: a lower layer located between 1.5 and 3.5 km and an upper layer extending between 3.0 and 6.0 km. The dust cloud is located above a well-structured boundary layer aerosol (evident in the lower part of figure 1 as a yellow and orange structure), which is found to start forming around 8:00 UTC, to reach its maximum height (~1500 m) around 15:00 UTC and to finally start decaying around 19:30 UTC.

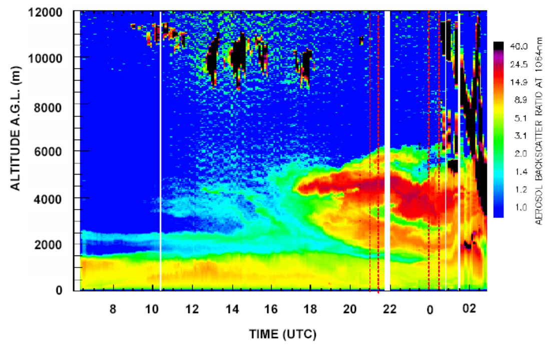

Figure 1. *Time evolution of the particle backscatter ratio at 1064 nm from 06:00 UTC on 1 August 2007 to 03:00 UTC on 2 August 2007.*

Figure 2 shows the time evolution of the water vapour mixing ratio from 18:45 UTC on 1 August 2007 to 03:16 UTC on 2 October 2005; the figure clearly reveals the appearance of a out-flow boundary in the final part of the measurement record, testified by the presence of a boundary region separating the thunderstorm-cooled air (outflow) from the surrounding air.

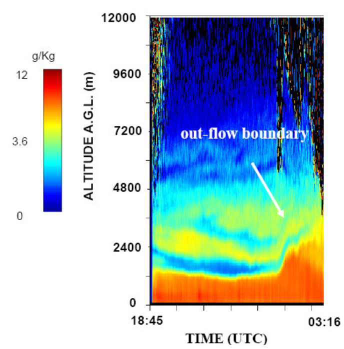

Figure 2. *Time evolution of the water vapour mixing ratio from 18:45 UTC on 1 August 2007 to 03:16 UTC on 2 August 2007.*

For the purpose of retrieving particle size distribution parameters as a function of altitude, we focused our attention on two specific times in the period when aerosol loading was higher, i.e. 21:00 UTC on 1 August 2007 and 00:00 UTC on 2 August. In order to get high enough signal-to-noise ratios for the retrieval scheme to be applicable, we considered half-hour averaging for both particle backscattering and extinction. The considered time intervals are represented by the red dashed lines in figure 1. Figure 3 shows the vertical profiles of the particle backscattering coefficient at 355, 532 and 1064 nm (left panel) and of the particle extinction coefficient at 355 and 532 nm (right panel) for 21:00-21:30 UTC on 1 August 2007, while figure 4 shows these same optical quantities for 00:00-00:30 UTC on 2 August 2007. Data in figures 6 and 7 are plotted with their error bars. In order to achieve comparable signal statistics, backscatter and extinction data are provided with different vertical resolutions (120 m and 300 m, respectively).

Figure 5 and 6 show the vertical profiles of particle depolarization at 355, $\delta_{par}^{355}(z)$, and of the extinction-to-backscatter ratio, or *lidar ratio,* at 355 nm ($S_{355}=\alpha_{355}/\beta_{355}$) and 532 nm ($S_{532}=\alpha_{532}/\beta_{532}$), for 21:00-21:30 UTC on 1 August 2007 and for 00:00-00:30 UTC on 2 August 2007, respectively.

For the purpose of applying the retrieval procedure, each optical quantity was averaged over layers of 300-400 m thickness. Figures 7 and 8 show the retrieved particle size distributions, expressed as *dV/dlnr*, for 21:00-21:30 UTC on 1 August 2007 and for 00:00-00:30 UTC on 2 August 2007, respectively. Results in these figures reveal the presence both in the lower and the upper dust layers of a fine mode with radii of 0.1-0.25 µm and of a coarse mode with radii of 1-6 µm. In the upper dust layer the coarse mode shows larger radii and dominates the distributions. Retrieved values of the fine and coarse mode radii are somewhat larger than those found in literature [11].

Figures 9 and 10 illustrate the variability with altitude of r_{mean}, r_{eff} and V for 21:00-21:30 UTC on 1 August 2007 and for 00:00-00:30 UTC on 2 August 2007, respectively. r_{mean} is in the range 0.09-0.16 µm, r_{eff} varies in the interval 0.1-1.4 µm, while V is in the range 6-80 µm^3/cm^3. More specifically, on 1 August 2007 r_{mean}, r_{eff} and V vary as a function of altitude from 0.1 µm, 0.2 µm and 6 µm^3/cm^3 at 1.7 km to 0.14 µm, 1.2 µm and 44 µm^3/cm^3 at 4.7 km, respectively. On 2 August 2007 r_{mean}, r_{eff} and V vary as a function of altitude in the range 0.11-0.15 µm, 0.2-1.4 µm and 8-80 µm^3/cm^3, respectively.

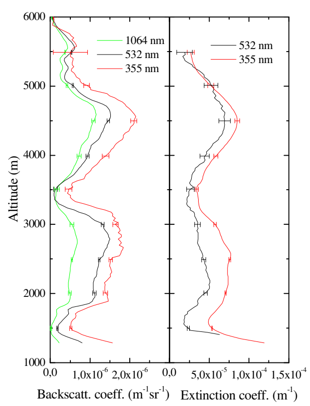

Figure 3. *Vertical profiles of particle backscattering coefficient at 355, 532 and 1064 nm (left panel) and particle extinction coefficient at 355 and 532 nm (right panel) for 21:00-21:30 UTC on 1 August 2007. All profiles are reported with their error bars.*

Figure 11 and 12 show the vertical profiles of N, m_r and m_i., for 21:00-21:30 UTC on 1 August 2007 and for 00:00-00:30 UTC on 2 August 2007, respectively. Values of N are in the range 150-1500 cm^{-3} on 1 August and in the range 400-1100 cm^3 on 2 August. The larger values observed on 1 August are associated with the larger dust loading characterizing the earlier stage of the dust outbreak event.

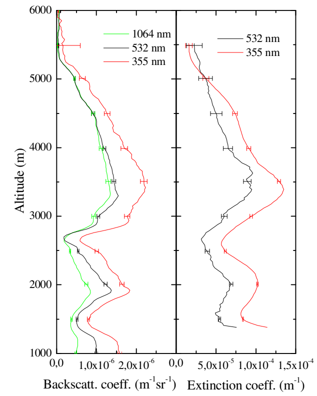

Figure 4. *Same as figure 3, but for 00:00-00:30 UTC on 2 August 2007.*

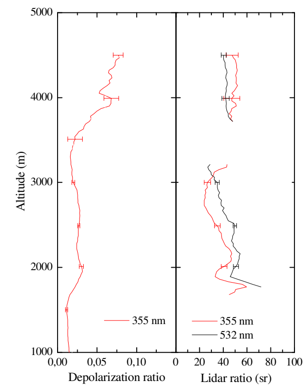

Figure 5. *Vertical profiles of* $\delta_{par}^{355}(z)$, *S_{355} and S_{532} for 21:00-21:30 UTC on 1 August 2007.*

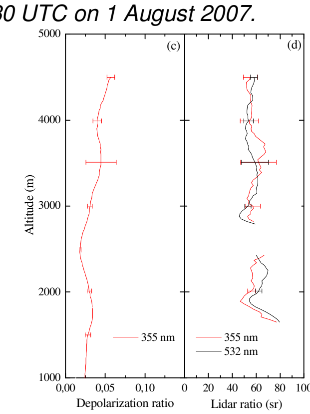

Figure 6. *Same as figure 5, but for 00:00-00:30 UTC on 2 August 2007.*

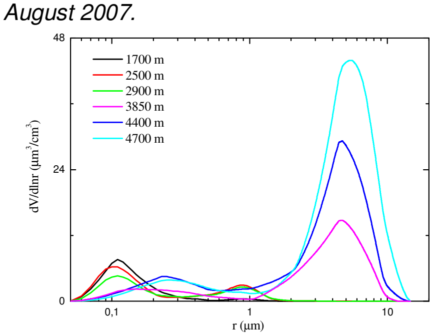

Figure 7. *Particle size distributions for 21:00-21:30 UTC on 1 August 2007. Different curves refer to different altitudes.*

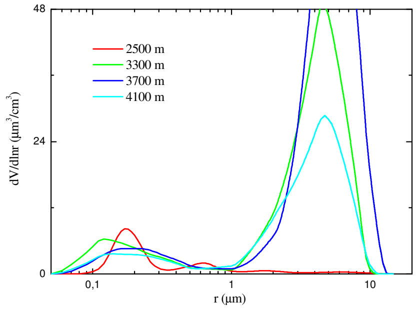

Figures 8. *Particle size distributions for 00:00-00:30 UTC on 2 August 2007. Different curves refer to different altitudes.*

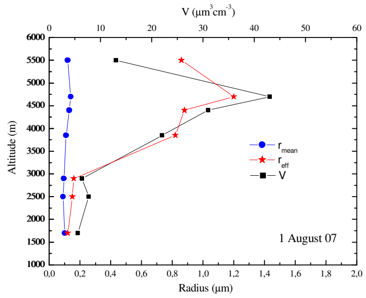

Figure 9. *Mean, effective particle radius and volume density for 21:00 UTC on 1 August.*

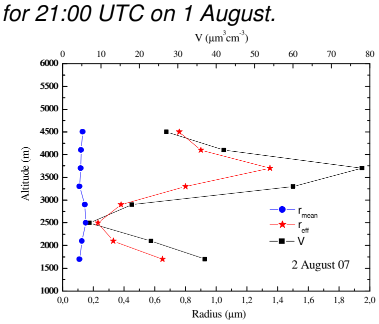

Figure 10. *Same as fugure 9, but for 00:00 UTC on 2 August 2007 (right panel).*

For what concerns the refractive index, values of m_r are in the range 1.45-1.62, and 0.005-0.012, respectively. Values of m_i are found to increase with altitude, while no evident trend with altitude is found in m_r. These values are compatible with literature values for Saharan dust particles [12]. More results from measurements and simulations will be illustrated and discussed at the Symposium.

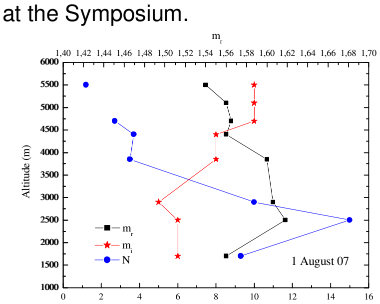

Figure 11: *Number density, real and imaginary part of the refractive index for 21:00 UTC on 1 August.*

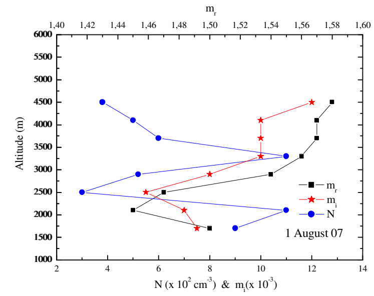

Figure 12: Same as fugure 9, but for 00:00-00:30 UTC on 2 August 2007.

REFERENCES

[1] Prospero, J. M., *et al.*, 2002: Environmental characterization of global sources of atmospheric soil dust identified with the Nimbus 7 total ozone mapping spectrometer (TOMS) absorbing aerosol product. *Rev. Geophys.*, **40,** 1002-1010.

[2] Moulin, C., et al., 1997: Control of atmospheric export of dust from North Africa by the North Atlantic Oscillation. *Nature*, **387**, 691–694.

[3] Swap, R. S., *et al.*, 1996: Temporal and spatial characteristics of Saharan dust outbreaks, *J. Geophys. Res.*, **101**, 4205–4220.

[4] Chiapello, I. and Moulin, C., 2002: TOMS and METEOSAT satellite records of the variability of Saharan dust transport over the Atlantic during the last two decades (1979–1997). *Geophys. Res. Lett.*, **29**, doi: 10.1029/2001GL013767.

[5] Chaboureau, *et al.*, Long-range transport of Saharan dust and its impact on precipitation forecast over western Europe, *J. Geophys. Res.*, submitted in July 2009.

[6] Di Girolamo, *et al.*, 2009: Rotational Raman Lidar measurements for the characterization of stratosphere-troposphere exchange mechanisms, *Journal of Atmospheric and Oceanic Technology*, Vol. 26, No. 9, 1742–1762.

[7] Müller, D., *et al.*, 2001: Comprehensive particle characterization from three-wavelength Raman lidar observations: case study, *Appl. Opt.*, **40**, 4863–4869.

[8] Veselovskii, .I., et al., 2002: Inversion with regularization for the retrieval of tropospheric aerosol parameters from multiwavelength lidar sounding, *Appl. Opt.*, **41**, 3685–3699.

[9] Mishchenko, M.I., *et al.*, 1997: Modeling phase functions for dustlike tropospheric aerosols using a mixture of randomly oriented polydisperse spheroids. *J. Geophys. Res.*, **102**, 16831-16847, doi:10.1029/96JD02110.

[10] Dubovik, O., *et al.*, 2007: Application of spheroids models to account for aerosol particle nonsphericity in remote sensing of desert dust, J*. Geophys.Res.*, **111**, doi:10.1029/2005JD00619.

[11] Dubovik, O., *et al.*, Variability of Absorption and Optical Properties of Key Aerosol Types Observed in Worldwide Location, J. Atmos. Sci., 59, 590–608, 2002.